Journal of Solid State Chemistry 182 (2009) 1921–1928

Contents lists available at ScienceDirect

Journal of Solid State Chemistry

journal homepage: www.elsevier.com/locate/jssc

Crystal structures of $RPt_{3-x}Si_{1-y}$ (R = Y, Tb, Dy, Ho, Er, Tm, Yb) studied by single crystal X-ray diffraction

Alexander Gribanov [a,b], Andriy Grytsiv [a], Peter Rogl [a,*], Yurii Seropegin [b], Gerald Giester [c]

[a] Institute of Physical Chemistry, University of Vienna, Währingerstrasse 42, A-1090 Wien, Austria
[b] Chemistry Department of the Moscow State University, Leninskie Gory, GSP-1, 119991 Moscow, Russia
[c] Institute of Mineralogy and Crystallography, University of Vienna, Althanstrasse 14, A-1090 Wien, Austria

ARTICLE INFO

Article history:
Received 12 December 2008
Received in revised form
31 March 2009
Accepted 3 May 2009
Available online 12 May 2009

Keywords:
Ternary silicides $RPt_{3-x}Si_{1-y}$
Single crystal
X-ray powder diffraction

ABSTRACT

The crystal structures of ternary compounds $RPt_{3-x}Si_{1-y}$(R = Y, Tb, Dy, Ho, Er, Tm, Yb) have been elucidated from X-ray single crystal CCD data. All compounds are isotypic and crystallize in the tetragonal space group $P4/mbm$. The general formula $RPt_{3-x}Si_{1-y}$ arises from defects: $x \approx 0.20$, $y \approx 0.14$. The crystal structure of $RPt_{3-x}Si_{1-y}$ can be considered as a packing of four types of building blocks which derive from the $CePt_3B$-type unit cell by various degrees of distortion and Pt, Si-defects.

1. Introduction

The discovery of $CePt_3Si$ as the first heavy fermion superconductor without inversion center (space group $P4mm$, $a = 0.4072$ nm, $c = 0.5442$ nm, $CePt_3B$-structure type [1,2]) has stimulated an intensive search for related intermetallic compounds exhibiting similar low temperature physical behavior [3]. In our previous studies [4] we have characterized physical properties of "light" rare earths RPt_3Si from La to Gd (except Eu), which are all isotypic and crystallize with the crystal structure of $CePt_3B$. Attempts to synthesize the members of the series with the remaining rare earth metals, however, prompted compounds with compositions close to RPt_3Si but with different crystal structures. Hitherto four intermetallics, $Er_{36}Pt_{102-x}Si_{32}$ ($x = 2.61$) [5], $Y_{18}Pt_{50+x}Si_{16-x}$ ($x = 0.28$), $Dy_{18}Pt_{50+x}Si_{16-x}$ ($x = 0.56$) [6], and $Yb_{18}Pt_{51.1}Si_{15.1}$ [7], were reported, which from X-ray single crystal studies were found to exhibit complicated disordered tetragonal crystal structures and a small but significant shift from the stoichiometric composition 1:3:1 (thus a formula $RPt_{3-x}Si_{1-y}$ is used in the current article). Whilst the compounds with Y, Dy, Yb adopt tetragonal crystal structures with space group $P4/mbm$ (no. 127) and similar atom distribution (parameters $a_0 \approx 1.870$ and $c_0 \approx 0.4065$ nm), the crystal structure of $Er_{36}Pt_{102-x}Si_{32}$ ($x = 2.61$) [5] is of a unique type with a two-fold superstructure in direction of the c-axis in space group $P4_2/mnm$ (no. 136) and with unit cell dimensions $a = 1.86723$ nm and $c = 0.81734\,\text{nm} \approx 2c_0$.

In the present work we focus on the single crystal structure evaluation for the Tb-, Ho-, and Tm-containing compounds as well as for Er from a new sample preparation. The new common crystal structure model, derived from these experimental data, is also applied to previously collected experimental data sets from single crystals of the Y-, Dy- [6], and Yb- [7] containing compounds.

2. Experimental techniques

The experimental techniques of preparation of single crystals and the X-ray structure investigation of $Y_{18}Pt_{50+x}Si_{16-x}$, $Dy_{18}Pt_{50+x}Si_{16-x}$, and $Yb_{18}Pt_{51.1}Si_{15.1}$ were already described in [6,7]. New alloys of $RPt_{3-x}Si_{1-y}$ (Tb, Dy, Ho, Er, Tm) of 1 g each were synthesized by arc-melting from high-purity elements (>99.9 mass%) on a water-cooled copper hearth in an argon environment starting from nominal composition $R_{21.5}Pt_{59.5}Si_{19.0}$ (at.%) in accordance with the composition derived earlier from a single crystal study of $Y_{18}Pt_{50+x}Si_{16-x}$ and $Dy_{18}Pt_{50+x}Si_{16-x}$ [6]. To ensure complete fusion, all alloys were re-melted three times. Due to high evaporation of Tm the corresponding alloy was prepared with excess of 1 mass % of the rare earth to compensate the losses. The as-cast alloys were vacuum-sealed in quartz tubes and annealed at 900 °C for 14 days before being quenched in cold water. These annealing conditions were chosen on the basis of our experience from previous studies of ternary systems: Yb–Pd–Si [8]

* Corresponding author. Fax: +43 1 4277 95245.
E-mail address: peter.franz.rogl@univie.ac.at (P. Rogl).

0022-4596/$ - see front matter © 2009 Elsevier Inc. All rights reserved.
doi:10.1016/j.jssc.2009.05.005

and Ce–Pt–Si [9]. For example, for Ce–Pt–Si alloys it was difficult to reach equilibrium at 600 °C even after long time annealing (1 month), whilst samples annealed at 800 °C for 2 weeks were found to be in equilibrium [9]. X-ray powder diffraction (XPD) data were collected employing a Guinier–Huber image plate system with Cu$K\alpha$1-radiation ($8^\circ < 2\theta < 100^\circ$) with Ge as a standard. Single crystals of Tb-, Ho-, Er-, and Tm-containing compounds were isolated from mechanically crushed alloys. High quality single crystals were pre-selected on an AXS-GADDS texture goniometer. Unit cell dimensions and Laue symmetry of the structures were determined prior to X-ray intensity (XSC) data collection on a four-circle Nonius Kappa diffractometer equipped with a CCD area detector and employing graphite monochromated Mo$K\alpha$ radiation ($\lambda = 0.071073$ nm). Orientation matrix and unit cell parameters were derived using program DENZO [10]. No absorption corrections were necessary because of the rather regular crystal shape and small dimensions of the investigated specimens. The structures were solved by direct methods and refined with the SHELXL-97 program [11]. GFourier [12] program was used for visualization of Fourier maps. Specimen compositions were determined by electron probe microanalysis (EPMA) on a Carl Zeiss DSM 962 instrument equipped with a Link EDX system operated at 20 kV and 60 μA.

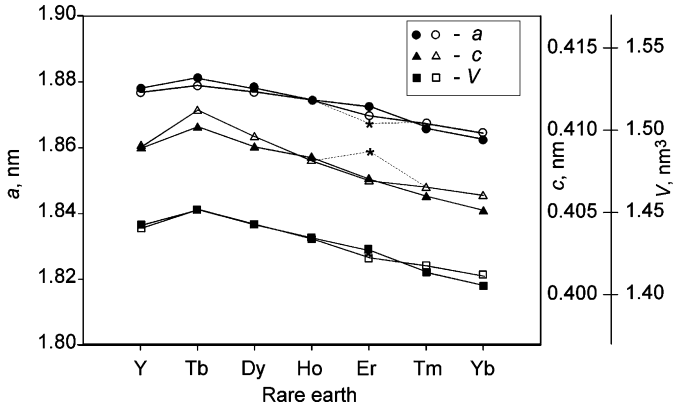

Fig. 1. Lattice parameters and cell volume for $RPt_{3-x}Si_{1-y}$. Filled symbols: XPD; open symbols: XSC; asterisks correspond to lattice parameters of $Er_{36}Pt_{102-z}Si_{32}$ ($z = 2.61$, $a = a_0$, $c = c_0/2$, $V = V_0/2$, Ref. [5]).

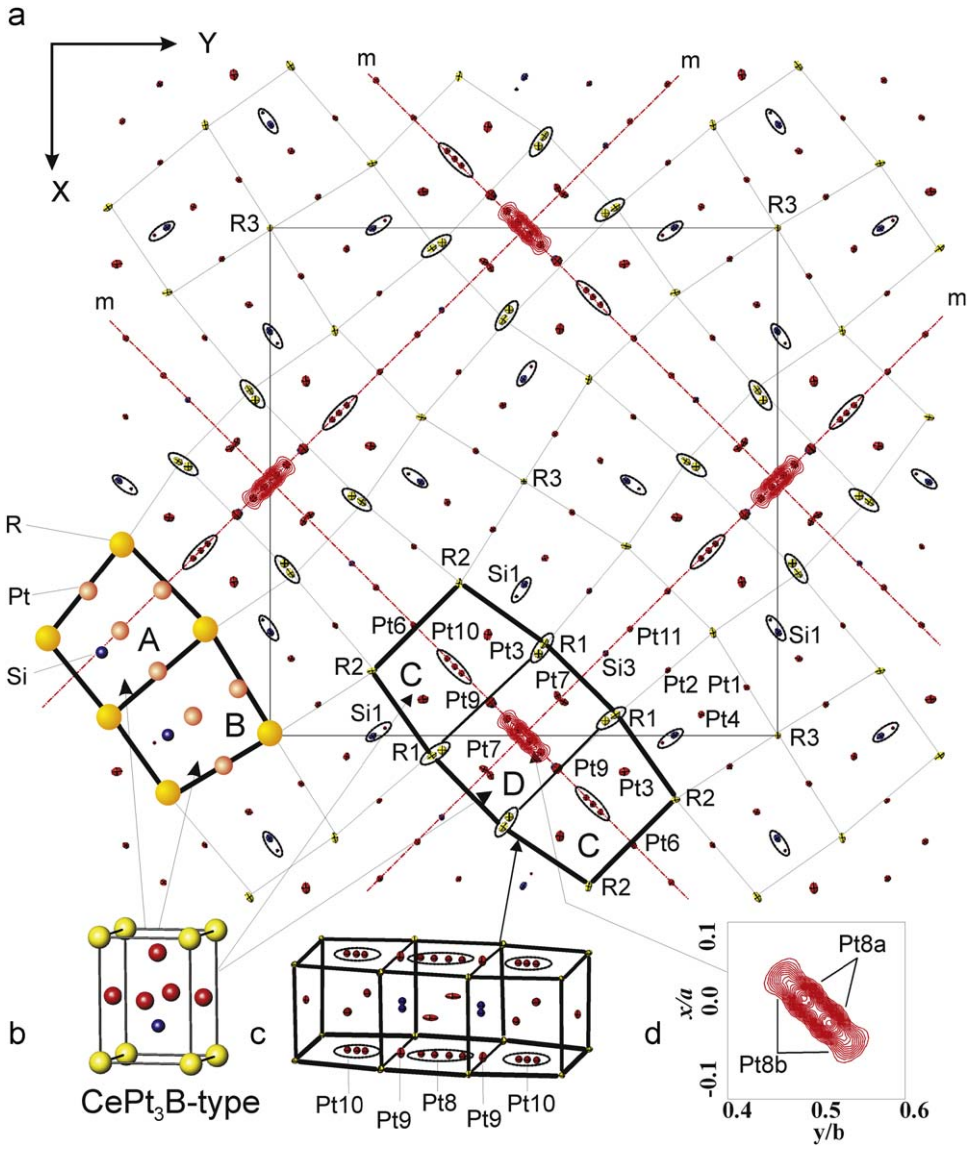

Fig. 2. Arrangement of atoms in $RPt_{3-x}Si_{1-y}$: (a) projection of the structure on xy plane, (b) unit cell of $CePt_3Si$ [1], (c) "problem area" C–D–C in $RPt_{3-x}Si_{1-y}$, and (d) electron density at $0, \frac{1}{2}, 0$ corresponding to Pt8a and Pt8b. For discussion see text.

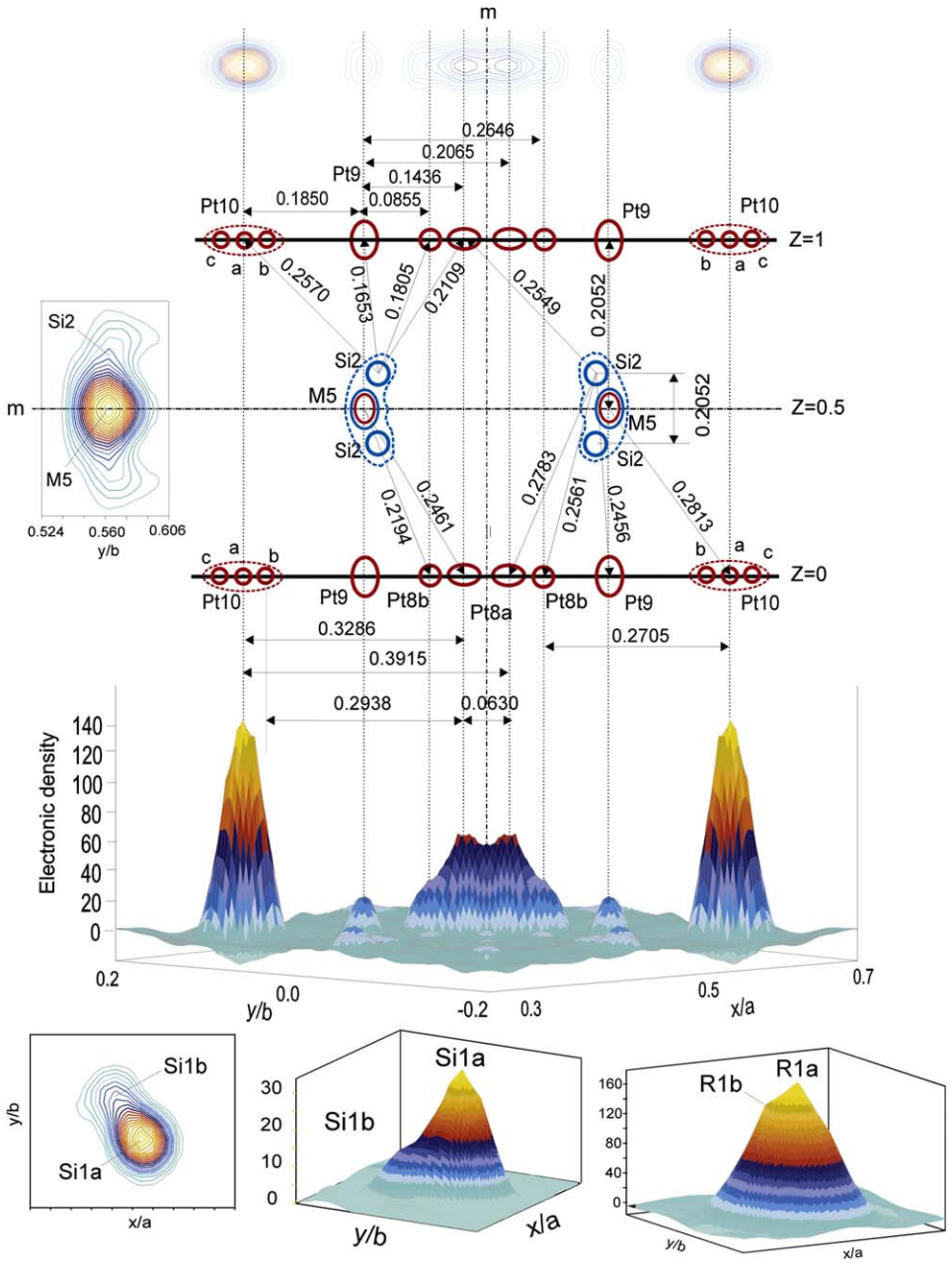

Fig. 3. Section of the unit cell of $RPt_{3-x}Si_{1-y}$ along the mirror plane (220) and electron densities for selected atoms in form of contour and surface plots. Electronic densities are given in $e^-/Å^3$. As an example data are given for the $TbPt_{3-x}Si_{1-y}$ compound (XSC). For details see discussion in the text.

3. Results and discussion

Lattice parameters, characteristic X-ray extinctions ($0\,k\,l$ for $k = 2n+1$ and $h\,0\,0$ for $h = 2n+1$) and X-ray intensities unambiguously documented that the crystal structures of $RPt_{3-x}Si_{1-y}$ for Tb, Ho, Er, and Tm compounds belong to the same structure type with tetragonal symmetry (space group $P4/mbm$ (no. 127). As the crystal structure seems to be close to the previously obtained structure solutions for $R_{18}Pt_{50+x}Si_{16-x}$ with $R = Y$, Dy [6] and $Yb_{18}Pt_{51.1}Si_{15.1}$ [7], the single crystal X-ray data sets are reinvestigated for all heavy rare earth members of the series $RPt_{3-x}Si_{1-y}$ ($R =$ Tb to Yb, Y).

Lattice parameters and crystal structure for $RPt_{3-x}Si_{1-y}$ are shown in Figs. 1–4 and crystallographic data are summarized in Tables 1–3. No doubling of the c-parameter was observed for our single crystal of $ErPt_{3-x}Si_{1-y}$. Fig. 5c shows X-ray diffraction peaks

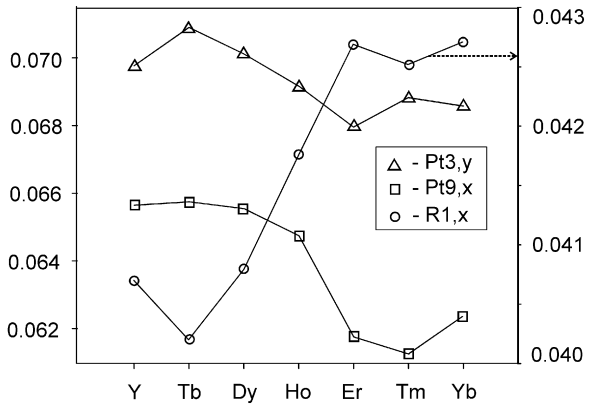

Fig. 4. Selected atomic parameters in $RPt_{3-x}Si_{1-y}$.

Table 1
Single crystal refinements for $RPt_{3-x}Si_{1-y}$ compounds.

Parameter/compound		$YPt_{3-x}Si_{1-y}$	$TbPt_{3-x}Si_{1-y}$	$DyPt_{3-x}Si_{1-y}$	$HoPt_{3-x}Si_{1-y}$	$ErPt_{3-x}Si_{1-y}$	$TmPt_{3-x}Si_{1-y}$	$YbPt_{3-x}Si_{1-y}$
Nominal composition (at.%)		$Y_{20}Pt_{60}Si_{20}$	$Tb_{21.5}Pt_{59.4}Si_{19.1}$	$Dy_{20}Pt_{60}Si_{20}$	$Ho_{21.5}Pt_{59.4}Si_{19.1}$	$Er_{21}Pt_{60}Si_{19}$	$Tm_{21.5}Pt_{59.4}Si_{19.1}$	$Yb_{21.5}Pt_{59.4}Si_{19.1}$
EPMA (± 1 at.%)		$Y_{22.1}Pt_{59.8}Si_{18.1}$	$Tb_{21.1}Pt_{61.6}Si_{16.3}$	$Dy_{21.4}Pt_{61.5}Si_{17.1}$	–	$Er_{20.3}Pt_{61.5}Si_{18.2}$	$Tm_{22.7}Pt_{60.0}Si_{16.8}$	$Yb_{22.8}Pt_{59.7}Si_{17.5}$
From refinement (at.%)		$Y_{21.4}Pt_{60.4}Si_{18.2}$	$Tb_{21.4}Pt_{60.4}Si_{18.2}$	$Dy_{21.4}Pt_{59.9}Si_{18.7}$	$Ho_{21.4}Pt_{60.1}Si_{18.4}$	$Er_{21.4}Pt_{60.4}Si_{18.2}$	$Tm_{21.4}Pt_{60.0}Si_{18.6}$	$Yb_{21.4}Pt_{59.5}Si_{19.1}$
Unit cell content (atoms)		$Y_{18}Pt_{50.76}Si_{15.24}$	$Tb_{18}Pt_{50.76}Si_{15.24}$	$Dy_{18}Pt_{50.32}Si_{15.68}$	$Ho_{18}Pt_{50.52}Si_{15.48}$	$Er_{18}Pt_{50.68}Si_{15.32}$	$Tb_{18}Pt_{50.36}Si_{15.64}$	$Tb_{18}Pt_{50.00}Si_{16.00}$
x; y in formula $RPt_{3-x}Si_{1-y}$		0.18; 0.15	0.18; 0.15	0.20; 0.13	0.19; 0.14	0.18; 0.15	0.20; 0.13	0.22; 0.11
Lattice parameters	a	1.8766 (2)	1.8787 (3)	1.8767 (2)	1.8742 (3)	1.8695 (2)	1.8671 (4)	1.8642 (7)
Powder data, (nm)	c	0.40898 (8)	0.41120 (9)	0.40956 (7)	0.4085 (3)	0.40692 (5)	0.4065 (1)	0.4060 (2)
Lattice parameters	a	1.87777 (3)	1.88099 (3)	1.87778 (2)	1.87415 (4)	1.87209 (3)	1.86574 (3)	1.86246 (3)
Single crystal data, (nm)	c	0.40891 (1)	0.41018 (1)	0.40897 (1)	0.40831 (1)	0.40701 (1)	0.40598 (1)	0.40513 (1)
Crystal size (μm)		$60 \times 60 \times 80$	$30 \times 30 \times 30$	$120 \times 30 \times 30$	$30 \times 30 \times 30$	$30 \times 30 \times 30$	$30 \times 30 \times 30$	$30 \times 30 \times 30$
Number of variables		96	99	96	99	99	99	101
Reflections in refinement		$1420 \geq 4\sigma$(Fo) of 1700	$1645 \geq 4\sigma$(Fo) of 1993	$1451 \geq 4\sigma$(Fo) of 1513	$1427 \geq 4\sigma$(Fo) of 1984	$1602 \geq 4\sigma$(Fo) of 1967	$1401 \geq 4\sigma$(Fo) of 1944	$1431 \geq 4\sigma$(Fo) of 1947
R_F^2		0.053	0.032	0.057	0.041	0.031	0.045	0.054
wR^2		0.138	0.070	0.150	0.097	0.067	0.105	0.132
GOF		1.031	1.075	1.136	1.053	0.951	1.050	1.109
Extinction		0.000009 (3)	0.00018 (1)	0.00009 (3)	0.00018 (2)	0.000161 (9)	0.00013 (2)	0.00008 (2)
R1a, 8i (x, y, 0)	x	0.0407 (1)	0.0402 (1)	0.04078 (7)	0.04175 (6)	0.04269 (5)	0.04252 (5)	0.04271 (6)
	y	0.3196 (1)	0.3192 (2)	0.31935 (8)	0.31887 (7)	0.31822 (5)	0.31861 (5)	0.31841 (6)
Occ.		1.0	0.93 (1)	1.0	0.96 (2)	0.92 (1)	1.0	1.0
$U_{eq.}$		0.0342 (7)	0.011 (4)	0.0266 (4)	0.0127 (3)	0.0138 (2)	0.0154 (3)	0.0161 (2)
R1b, 8i (x, y, 0)	x	–	0.029 (1)	–	0.026 (2)	0.0300 (6)	–	–
(x, y, 0)	y	–	0.339 (2)	–	0.343 (2)	0.3375 (6)	–	–
Occ.		–	0.07 (1)	–	0.04 (2)	0.08 (1)	–	–
$U_{eq.}$		–	0.012 (3)	–	0.011 (5)	0.016 (2)	–	–
R2, 8i (x, y, 0)	x	0.2020 (1)	0.20176 (4)	0.20211 (7)	0.20267 (5)	0.2032213)	0.20235 (5)	0.20212 (6)
Occ = 1.0	y	0.1263 (1)	0.12715 (3)	0.12660 (7)	0.12591 (5)	0.12523 (3)	0.12570 (5)	0.12570 (6)
$U_{eq.}$		0.0263 (4)	0.0097 (1)	0.0216 (3)	0.0098 (2)	0.0108 (1)	0.0120 (2)	0.0151 (2)
R3, 2a (0, 0, 0) occ.; $U_{eq.}$		1.0; 0.0225 (6)	1.0; 0.0056 (2)	1.0; 0.0171 (4)	1.0; 0.0053 (3)	1.0; 0.0066 (2)	1.0; 0.0065 (3)	1.0; 0.0078 (3)
Pt1, 8j (x, y, $\frac{1}{2}$)	x	0.09495 (4)	0.09458 (2)	0.09476 (5)	0.09500 (4)	0.09530 (2)	0.09535 (4)	0.09538 (4)
Occ. = 1.0	y	0.06033 (4)	0.06104 (2)	0.06035 (5)	0.05980 (4)	0.05925 (2)	0.05960 (4)	0.05944 (4)
$U_{eq.}$		0.0228 (2)	0.0062 (1)	0.0177 (2)	0.0059 (2)	0.0072 (1)	0.0071 (2)	0.0087 (2)
Pt2, 8j (x, y, $\frac{1}{2}$)	x	0.12914 (4)	0.12825 (2)	0.12904 (5)	0.12978 (4)	0.13072 (2)	0.13005 (4)	0.13009 (5)
Occ. = 1.0	y	0.21544 (4)	0.21606 (2)	0.21545 (5)	0.21474 (4)	0.21411 (2)	0.21450 (4)	0.21432 (4)
$U_{eq.}$		0.0228 (2)	0.0060 (1)	0.0175 (3)	0.0058 (2)	0.00711 (9)	0.0073 (2)	0.0097 (2)
Pt3, 8j (x, y, $\frac{1}{2}$)	x	0.30178 (5)	0.30164 (3)	0.30200 (6)	0.30297 (5)	0.30310 (3)	0.30513 (6)	0.30553 (7)
Occ. = 1.0	y	0.06979 (5)	0.07093 (3)	0.07014 (6)	0.06919 (4)	0.06798 (3)	0.06885 (5)	0.06860 (6)
$U_{eq.}$		0.0321 (2)	0.0149 (1)	0.0265 (3)	0.0161 (2)	0.0179 (1)	0.0220 (2)	0.0247 (3)
Pt4, 8i (x, y, 0)	x	0.04225 (4)	0.04141 (3)	0.04189 (5)	0.04236 (4)	0.04317 (3)	0.04210 (4)	0.04205 (5)
Occ. = 1.0	y	0.15046 (4)	0.15080 (3)	0.15047 (5)	0.15017 (4)	0.14987 (3)	0.15032 (4)	0.15028 (5)
$U_{eq.}$		0.0235 (2)	0.0068 (1)	0.0182 (2)	0.0067 (2)	0.00778 (9)	0.0080 (2)	0.0103 (2)
Pt6, 4h (x, $\frac{1}{2}+x$, $\frac{1}{2}$)	x	0.21580 (4)	0.21677 (3)	0.21615 (5)	0.21513 (4)	0.21425 (3)	0.21488 (4)	0.21487 (5)
Occ. = 1.0; $U_{eq.}$		0.0259 (2)	0.0091 (1)	0.0209 (3)	0.0087 (2)	0.0098 (1)	0.0107 (2)	0.0133 (3)

Pt7, 8*j* (x, y, $\frac{1}{2}$)	x	0.5789 (2)	0.5784 (1)	0.5786 (3)	0.5790 (2)	0.57998 (8)	0.5796 (1)	0.5797 (1)
Occ. = 0.5	y	0.0662 (2)	0.0660 (1)	0.0658 (2)	0.0658 (2)	0.06589 (7)	0.0642 (1)	0.0636 (1)
$U_{eq.}$		0.0278 (9)	0.0098 (5)	0.022 (1)	0.0108 (7)	0.0114 (4)	0.0138 (6)	0.0152 (6)
Pt8a, 4*g* (x, $\frac{1}{2}+x$, 0)	x	0.0117 (2)	0.0119 (1)	0.0122 (3)	0.0120 (1)	0.0110 (1)	0.0123 (2)	0.0153 (3)
Occ.		0.320 (8)	0.32 (3)	0.30 (1)	0.32 (1)	0.33 (1)	0.34 (1)	0.31 (1)
$U_{eq.}$		0.0255 (8)	0.0095 (5)	0.019 (1)	0.0092 (6)	0.0052 (4)	0.0178 (8)	0.024 (2)
Pt8b, 4*g* (x, $\frac{1}{2}+x$, 0)	x	0.0333 (5)	0.0337 (2)	0.0335 (5)	0.0335 (3)	0.0286 (3)	0.0347 (5)	0.0411 (8)
Occ.		0.180 (8)	0.18 (3)	0.20 (1)	0.18 (1)	0.17 (1)	0.16 (1)	0.19 (1)
U_{iso}		0.033 (2)	0.012 (1)	0.023 (2)	0.018 (1)	0.007 (1)	0.014 (2)	0.040 (4)
Pt9, 4*g* (x, $\frac{1}{2}+x$, 0)	x	0.0657 (4)	0.0658 (2)	0.0656 (4)	0.0648 (3)	0.0618 (3)	0.0611 (3)	0.0624 (3)
Occ.		0.158 (5)	0.157 (3)	0.210 (7)	0.201 (4)	0.212 (3)	0.284 (5)	0.280 (6)
$U_{eq.}$		0.037 (2)	0.014 (1)	0.035 (2)	0.021 (2)	0.033 (1)	0.028 (2)	0.027 (2)
Pt10a, 4*g* (x, $\frac{1}{2}+x$, 0)	x	0.134 (1)	0.1353 (5)	0.131 (2)	0.1362 (6)	0.1345 (7)	0.134 (1)	0.1354 (7)
Occ.		0.51 (2)	0.464 (8)	0.47 (2)	0.41 (2)	0.45 (2)	0.44 (3)	0.43 (2)
U_{iso}		0.0230 (5)	0.0060 (3)	0.0150 (6)	0.0066 (4)	0.0066 (3)	0.0088 (5)	0.0120 (6)
Pt10b, 4*g* (x, $\frac{1}{2}+x$, 0)	x	0.122 (1)	0.1223 (4)	0.119 (2)	0.1247 (5)	0.1239 (6)	0.123 (1)	0.1233 (9)
Occ.		0.26 (4)	0.32 (2)	0.16 (5)	0.37 (3)	0.28 (3)	0.21 (5)	0.23 (3)
U_{iso}		0.0230 (5)	0.0060 (3)	0.0150 (6)	0.0066 (4)	0.0066 (3)	0.0088 (5)	0.0120 (6)
Pt10c, 4*g* (x, $\frac{1}{2}+x$, 0)	x	0.148 (3)	0.150 (2)	0.144 (2)	0.156 (3)	0.148 (2)	0.148 (3)	0.154 (2)
Occ.		0.07 (3)	0.06 (1)	0.16 (4)	0.024 (7)	0.05 (2)	0.07 (2)	0.061 (9)
U_{iso}		0.0230 (5)	0.0060 (3)	0.0150 (6)	0.0066 (4)	0.0066 (3)	0.0088 (5)	0.0120 (6)
Pt11, 4*g* (x, $\frac{1}{2}+x$, 0)	x	0.70985 (4)	0.70935 (2)	0.70987 (5)	0.71049 (4)	0.71122 (2)	0.71044 (4)	0.71039 (5)
Occ. = 1.0; $U_{eq.}$		0.0231 (2)	0.0060 (1)	0.0179 (3)	0.0058 (2)	0.0070 (1)	0.0070 (2)	0.0089 (2)
Si1a, 8*j* (x, y, $\frac{1}{2}$)	x	0.0021 (4)	0.0014 (2)	0.0018 (5)	0.0030 (3)	0.0033 (2)	0.0019 (4)	0.0023 (5)
	y	0.2029 (4)	0.2026 (3)	0.2025 (5)	0.2032 (3)	0.2038 (2)	0.2045 (3)	0.2048 (4)
Occ.		0.96 (4)	0.94 (2)	0.96 (1)	0.97 (1)	0.96 (1)	0.96 (1)	0.94 (1)
$U_{eq.}$		0.024 (1)	0.007 (1)	0.018 (1)	0.013 (1)	0.0081 (6)	0.020 (1)	0.010 (1)
Si1b, 8*j* (x, y, $\frac{1}{2}$)	x	−0.015 (1)	−0.0139 (7)	−0.011 (1)	−0.016 (1)	−0.0144 (7)	−0.020 (2)	−0.016 (2)
	y	0.229 (1)	0.2263 (7)	0.228 (1)	0.226 (1)	0.2287 (7)	0.233 (2)	0.228 (3)
Occ.		0.04 (4)	0.06 (2)	0.04 (1)	0.03 (1)	0.04 (1)	0.04 (1)	0.06 (1)
U_{iso}		0.014 (3)	0.005 (2)	0.013 (4)	0.007 (4)	0.006 (2)	0.009 (5)	0.018 (7)
Si2, 8*k* (x, $\frac{1}{2}+x$, z)	x	0.0611 (8)	0.0612 (6)	0.060 (2)	0.062 (1)	0.0609 (7)	0.060 (1)	0.059 (2)
	z	0.416 (7)	0.402 (4)	0.407 (5)	0.379 (7)	0.395 (5)	0.357 (8)	0.390 (9)
Occ.		0.34 (1)	0.28 (2)	0.22 (4)	0.22 (3)	0.24 (2)	0.19 (3)	0.20 (4)
U_{iso}		0.019 (6)	0.007 (4)	0.014 (8)	0.008 (7)	0.008 (5)	0.008 (8)	0.013 (9)
M5, 4*h* (x, $\frac{1}{2}+x$, $\frac{1}{2}$)	x	0.0629 (2)	0.0630 (2)	0.0631 (4)	0.0626 (3)	0.0623 (2)	0.0629 (4)	0.0634 (8)
Occ.		0.19 (2)Pt+0.13Si	0.19 (2)Pt+0.25 Si	0.08 (3)Pt+0.48 Si	0.13 (2)Pt+0.43Si	0.17 (3)Pt+0.35Si	0.09 (3)Pt+0.53 (3)Si	0.60 (4)Si
$U_{eq.}$		0.020 (2)	0.0050 (8)	0.008 (2)	0.006 (1)	0.0081 (9)	0.019 (2)	0.016 (4)
Si3, 4*h* (x, $\frac{1}{2}+x$, $\frac{1}{2}$)	x	0.6617 (3)	0.6613 (2)	0.6617 (4)	0.6615 (3)	0.6619 (2)	0.6612 (3)	0.6611 (4)
Occ.		1.0	1.0	1.0	1.0	1.0	1.0	1.0
$U_{eq.}$		0.026 (2)	0.0062 (8)	0.017 (2)	0.011 (1)	0.0059 (8)	0.013 (2)	0.010 (2)
Residual density; e/Å,	max	6.13	5.26	7.42	6.44	4.96	8.17	10.73
	min	−4.05	−8.92	−6.06	−8.91	−8.63	−8.37	−11.98

Space group *P*4/*mbm*, no. 127, atomic displacement parameters, $U_{eq.}$ and $U_{iso.}$ are given in $10^2\,nm^2$.

Table 2
Anisotropic atomic displacement parameters in the structures $R\mathrm{Pt}_{3-x}\mathrm{Si}_{1-y}$ (in $10^2\,\mathrm{nm}^2$), $U_{23} = U_{13} = 0$ in accordance with symmetry.

Site		Y	Tb	Dy	Ho	Er	Tm	Yb
*R*1a	U_{11}	0.030 (1)	0.0105 (5)	0.0270 (7)	0.0087 (5)	0.0121 (3)	0.0123 (5)	0.0159 (5)
	U_{22}	0.037 (1)	0.0145 (5)	0.0336 (7)	0.0128 (6)	0.0150 (4)	0.0149 (5)	0.0177 (5)
	U_{33}	0.036 (1)	0.0105 (3)	0.0192 (6)	0.0165 (5)	0.0143 (3)	0.0190 (6)	0.0148 (5)
	U_{12}	−0.0112 (9)	−0.0054 (5)	−0.0081 (5)	−0.0062 (4)	−0.0058 (3)	−0.0074 (3)	−0.0061 (4)
*R*1b	U_{iso}	–	0.012 (3)	–	0.011 (5)	0.015 (2)	–	–
*R*2	U_{11}	0.0290 (9)	0.0158 (3)	0.0286 (6)	0.0145 (4)	0.0164 (3)	0.0191 (5)	0.0266 (5)
	U_{22}	0.0219 (8)	0.0065 (2)	0.0207 (5)	0.0043 (3)	0.0078 (2)	0.0064 (4)	0.0117 (4)
	U_{33}	0.0281 (9)	0.0067 (3)	0.0154 (5)	0.0106 (4)	0.0083 (3)	0.0106 (5)	0.0068 (5)
	U_{12}	0.0029 (7)	0.0021 (2)	0.0027 (4)	0.0025 (3)	0.0021 (2)	0.0017 (3)	0.0016 (4)
*R*3	U_{11}	0.0197 (9)	0.0058 (3)	0.0185 (5)	0.0031 (4)	0.0061 (3)	0.0053 (4)	0.0096 (4)
	U_{22}	0.0197 (9)	0.0058 (3)	0.0185 (5)	0.0031 (4)	0.0061 (3)	0.0053 (4)	0.0096 (4)
	U_{33}	0.028 (2)	0.0053 (5)	0.0144 (9)	0.0097 (7)	0.0076 (5)	0.0089 (8)	0.0044 (8)
	U_{12}	0.0000 (0)	0.0000 (0)	0.0000 (0)	0.0000 (0)	0.0000 (0)	0.0000 (0)	0.0000 (0)
Pt1	U_{11}	0.0197 (3)	0.0058 (2)	0.0197 (4)	0.0038 (3)	0.0069 (2)	0.0054 (3)	0.0108 (4)
	U_{22}	0.0201 (3)	0.0063 (2)	0.0200 (4)	0.0039 (3)	0.0068 (2)	0.0059 (3)	0.0108 (3)
	U_{33}	0.0286 (4)	0.0064 (2)	0.0134 (4)	0.0100 (3)	0.0079 (2)	0.0101 (4)	0.0044 (4)
	U_{12}	0.0006 (2)	0.0007 (1)	0.0006 (3)	0.0005 (2)	0.0007 (1)	0.0002 (2)	0.0001 (2)
Pt2	U_{11}	0.0194 (3)	0.0052 (2)	0.0188 (4)	0.0033 (3)	0.0065 (2)	0.0059 (3)	0.0123 (4)
	U_{22}	0.0202 (3)	0.0058 (2)	0.0189 (4)	0.0034 (3)	0.0065 (2)	0.0056 (3)	0.0105 (4)
	U_{33}	0.0289 (4)	0.0070 (2)	0.0149 (4)	0.0107 (3)	0.0083 (3)	0.0105 (4)	0.0063 (4)
	U_{12}	−0.0010 (2)	−0.0013 (1)	−0.0009 (3)	−0.0011 (2)	−0.0014 (1)	−0.0020 (2)	−0.0031 (3)
Pt3	U_{11}	0.0337 (4)	0.0191 (3)	0.0322 (5)	0.0178 (4)	0.0218 (3)	0.0244 (5)	0.0297 (5)
	U_{22}	0.0255 (4)	0.0108 (2)	0.0241 (5)	0.0087 (3)	0.0124 (2)	0.0127 (4)	0.0187 (5)
	U_{33}	0.0371 (5)	0.0148 (3)	0.0232 (5)	0.0219 (4)	0.0196 (3)	0.0288 (6)	0.0258 (6)
	U_{12}	−0.0006 (3)	0.0009 (2)	0.0002 (4)	−0.0007 (3)	−0.0016 (2)	−0.0028 (3)	−0.0031 (4)
Pt4	U_{11}	0.0229 (3)	0.0083 (2)	0.0224 (4)	0.0061 (3)	0.0092 (2)	0.0086 (3)	0.0151 (4)
	U_{22}	0.0205 (3)	0.0066 (2)	0.0201 (4)	0.0047 (3)	0.0075 (2)	0.0064 (3)	0.0114 (4)
	U_{33}	0.0271 (4)	0.0055 (2)	0.0120 (4)	0.0093 (3)	0.0067 (2)	0.0090 (4)	0.0043 (4)
	U_{12}	−0.0008 (2)	−0.0006 (1)	−0.0010 (3)	−0.0009 (2)	−0.0010 (1)	−0.0020 (2)	−0.0029 (3)
Pt6	U_{11}	0.0209 (3)	0.0067 (2)	0.0199 (4)	0.0046 (3)	0.0075 (2)	0.0068 (3)	0.0126 (3)
	U_{22}	0.0209 (3)	0.0067 (2)	0.0199 (4)	0.0046 (3)	0.0075 (2)	0.0068 (3)	0.0126 (3)
	U_{33}	0.0357 (6)	0.0141 (3)	0.0229 (7)	0.0170 (5)	0.0145 (3)	0.0185 (6)	0.0146 (7)
	U_{12}	0.0015 (3)	0.0011 (2)	0.0011 (4)	0.0006 (3)	0.0004 (2)	0.0003 (3)	0.0000 (4)
Pt7	U_{11}	0.028 (2)	0.0130 (9)	0.027 (2)	0.011 (1)	0.0133 (7)	0.014 (1)	0.018 (1)
	U_{22}	0.025 (1)	0.0084 (8)	0.023 (2)	0.008 (1)	0.0104 (7)	0.012 (1)	0.016 (1)
	U_{33}	0.0301 (6)	0.0079 (3)	0.0153 (6)	0.0132 (5)	0.0105 (4)	0.0150 (7)	0.0112 (7)
	U_{12}	−0.005 (1)	−0.0029 (8)	−0.003 (2)	−0.005 (1)	−0.0035 (6)	−0.004 (1)	−0.002 (1)
Pt8a	U_{11}	0.023 (1)	0.0100 (8)	0.022 (2)	–	0.0036 (7)	–	0.033 (3)
	U_{22}	0.023 (1)	0.0100 (8)	0.022 (2)	–	0.0036 (7)	–	0.033 (3)
	U_{33}	0.030 (2)	0.0086 (9)	0.013 (2)	–	0.008 (1)	–	0.005 (2)
	U_{12}	0.005 (2)	0.004 (1)	0.003 (3)	–	−0.002 (1)	–	0.027 (3)
	U_{iso}	–	–	–	0.0092 (6)		0.0178 (8)	–
Pt8b	U_{iso}	0.033 (2)	0.012 (1)	0.023 (2)	0.018 (1)	0.007 (1)	0.014 (2)	0.040 (4)
Pt9	U_{11}	0.032 (3)	0.011 (2)	0.035 (3)	0.018 (2)	0.041 (2)	0.022 (2)	0.024 (2)
	U_{22}	0.032 (3)	0.011 (2)	0.035 (3)	0.018 (2)	0.041 (2)	0.022 (2)	0.024 (2)
	U_{33}	0.046 (5)	0.021 (2)	0.035 (4)	0.026 (3)	0.018 (2)	0.040 (4)	0.032 (4)
	U_{12}	−0.003 (3)	−0.004 (2)	−0.001 (3)	0.006 (2)	−0.025 (2)	0.007 (2)	0.002 (2)
Pt10a	U_{iso}	0.0230 (5)	0.0060 (3)	0.0150 (6)	0.0066 (4)	0.0066 (3)	0.0088 (5)	0.0120 (6)
Pt10b	U_{iso}	0.0230 (5)	0.0060 (3)	0.0150 (6)	0.0066 (4)	0.0066 (3)	0.0088 (5)	0.0120 (6)
Pt10c	U_{iso}	0.0230 (5)	0.0060 (3)	0.0150 (6)	0.0066 (4)	0.0066 (3)	0.0088 (5)	0.0120 (6)
Pt11	U_{11}	0.0211 (3)	0.0066 (2)	0.0207 (4)	0.0045 (3)	0.0074 (2)	0.0069 (3)	0.0116 (3)
	U_{22}	0.0211 (3)	0.0066 (2)	0.0207 (4)	0.0045 (3)	0.0074 (2)	0.0069 (3)	0.0116 (3)
	U_{33}	0.0273 (5)	0.0049 (3)	0.0123 (6)	0.0084 (4)	0.0061 (3)	0.0071 (5)	0.0033 (5)
	U_{12}	0.0004 (3)	0.0006 (2)	0.0007 (4)	0.0009 (3)	0.0005 (2)	0.0013 (3)	0.0021 (4)
Si1a	U_{11}	0.023 (3)	0.007 (2)	0.024 (3)	0.009 (3)	0.008 (2)	0.024 (3)	0.015 (3)
	U_{22}	0.021 (3)	0.007 (2)	0.015 (3)	0.010 (3)	0.009 (2)	0.013 (3)	0.006 (3)
	U_{33}	0.030 (3)	0.008 (2)	0.016 (3)	0.019 (3)	0.006 (2)	0.023 (3)	0.009 (3)
	U_{12}	−0.003 (2)	−0.002 (2)	−0.002 (3)	−0.001 (2)	−0.003 (1)	−0.006 (2)	0.00 (3)
Si1b	U_{iso}	0.014 (3)	0.005 (2)	0.013 (4)	0.007 (4)	0.006 (2)	0.009 (5)	0.018 (7)
Si2	U_{iso}	0.019 (6)	0.007 (4)	0.014 (8)	0.008 (7)	0.007 (5)	0.008 (8)	0.013 (9)
M5	U_{11}	0.023 (4)	0.005 (2)	0.007 (4)	0.006 (2)	0.009 (2)	0.019 (4)	0.018 (8)
	U_{22}	0.023 (4)	0.005 (2)	0.007 (4)	0.006 (2)	0.009 (2)	0.019 (4)	0.018 (8)
	U_{33}	0.014 (6)	0.004 (2)	0.010 (7)	0.006 (5)	0.007 (3)	0.020 (7)	0.01 (1)
	U_{12}	−0.001 (2)	0.001 (1)	−0.000 (2)	−0.003 (2)	−0.001 (1)	−0.006 (3)	−0.005 (6)
Si3	U_{11}	0.021 (2)	0.005 (1)	0.018 (2)	0.007 (2)	0.005 (1)	0.008 (2)	0.009 (2)
	U_{22}	0.021 (2)	0.005 (1)	0.018 (2)	0.007 (2)	0.005 (1)	0.008 (2)	0.009 (2)
	U_{33}	0.035 (4)	0.008 (2)	0.016 (4)	0.018 (4)	0.004 (2)	0.024 (5)	0.013 (5)
	U_{12}	0.001 (3)	0.000 (2)	0.000 (3)	0.002 (2)	−0.003 (2)	−0.002 (3)	0.002 (3)

assembled from all the frames in the form of a rotation photograph about the *c*-axis. The observed picture unambiguously defines a *c*-parameter of ~0.41 nm. Consequently the crystal structure of $Er_{36}Pt_{102-x}Si_{32}$ ($x = 2.61$) (space group $P4_2/mnm$, $Z = 1$, $a = 1.86723(1)$, $c = 0.81734(1)$ nm), as previously reported by Tursina et al. [5] with twice the *c*-parameter, is considered a polymorphic modification. The lattice parameters for $YPt_{3-x}Si_{1-y}$ are close to those of $DyPt_{3-x}Si_{1-y}$, while the general trend of the cell dimensions within the rare earths series reflects the conventional lanthanoid contraction (see Fig. 1). For the polymorph $Er_{36}Pt_{102-x}Si_{32}$ small deviations from the trend are encountered, i.e. the *a*-parameter is slightly smaller whilst the *c*-parameter ($c = c_0/2$) is significantly bigger than for $ErPt_{3-x}Si_{1-y}$.

Fine-tuning of the structural model particularly for the regions with atom disorder was performed with help of difference Fourier maps in combination with the analyses of interatomic distances and site occupation factors. All crystallographic sites were refined with anisotropic atomic displacement parameters (ADP), except for Si2 and Pt8b positions, which are very close to M5 and Pt8a, as well as Pt8a atoms for Ho-, Er-, and Tm-compounds (for details see below). Additional weak electronic densities near atoms R1, Si1, and Si3 were also refined in isotropic approximation (see Table 2). For easy comparison with the previous paper [6] labeling of the crystallographic sites in Table 1 closely follows the list given in [6] and no additional standardization procedure was attempted. As most of the crystallographic sites and corresponding atomic coordinates coincide with those reported before [6], coordination polyhedra are similar to those described earlier [6,7].

Fig. 2 illustrates the atomic arrangement in a projection on the *xy* plane. The structure can be presented as a packing of building blocks related to the $CePt_3B$-type unit cell (Fig. 2b). Two slightly distorted building blocks with exact composition 1:3:1 (Fig. 2a, A and B,) and two strongly distorted blocks deficient in silicon and platinum (Fig. 2a, C and D) are outlined as the main construction elements of the crystal structure of $RPt_{3-x}Si_{1-y}$. No doubt exists about the basic framework constructed with fragments A and B, whereas the area (C+D+C) needed to be carefully analyzed, because of two reasons: (i) strong anisotropy of electron densities that are located in close distances, (ii) partial occupancies and statistical distribution of atoms within that area. For a 3D view on the area composed of fragments C+D+C see Fig. 2c. A Fourier-map around $(0,\frac{1}{2},0)$ is shown in Fig. 2d representing the center "problem" area. The problems essentially arise in the space around sites Pt9–Pt10–Pt8a–Pt8b–M5 being not fully occupied. With the aid of differential Fourier-maps the electronic density distribution in the space between Pt9 atoms were found to be very similar for all $RPt_{3-x}Si_{1-y}$ intermetallics. The distributions of electronic densities around atoms *R*1 and Si1 were also very similar for all compounds in the series. As a typical example such a map is presented for $TbPt_{3-x}Si_{1-y}$ in Fig. 2d. From this map one can see the existence of four maxima, being correlated by a mirror plane in two atom sites, Pt8a–Pt8b. Fig. 3 shows the atom arrangement in the "problem" area within the mirror plane (220) and in addition the corresponding Fourier-maps are given. Independent refinement of site occupancy for Pt8a and Pt8b sums up to 1 without constraints. A similar situation is met for Pt9 and Pt10. Short interatomic distances Pt8a–Pt8b (0.0581 nm) and Pt9–Pt10 (0.1850 nm) do not allow these pairs of atoms to exist simultaneously. Additional electron density near Pt10 requests the insertion of two more sites, Pt10b and Pt10c. A related situation concerns atoms M5 and Si2. The refinement of positions M5 and Si2 was satisfactorily performed based on three arguments: (1) both sites are not fully occupied and the sum of their occupancies is equal to 1; (2) the M5 site comprises a random mix of Si and Pt atoms; (3) the site Si2 is occupied by Si only. In all three cases, Pt8a–Pt8b, Pt9–Pt10, and M5–Si2, we encounter an occupancy of 1 for each of the pairs, which leads us to conceive each of these atom groups as one "physical atom" forming a hypothetical base structure. The real and strongly disturbed atom arrangement in this problem area exerts further imperfections to the near surroundings. Thus an additional electron density was noticed near Si1 for all compounds and near R1 for the Tb, Ho, and Er representatives. These densities are shown at the bottom line of Fig. 3 in the form of contour and surface plots. The electron densities were described as atoms Si1b and R1b, respectively. Finally, summing up all occupancies yields for all compounds a structural chemical formula $RPt_{3-x}Si_{1-y}$ ($x \approx 0.17$–0.22, $y \approx 0.11$–0.16) in good agreement with EPMA data (see Table 3).

Analysis of the positional parameters in all compounds $RPt_{3-x}Si_{1-y}$ (see Table 1) reflects a monotonic trend following the lanthanoid contraction and positional parameter changes (from Tb to Yb) stay below 3% with exception for the atoms R1, Pt3 and Pt9 (6, 4 and 8%, respectively; see Fig. 4).

Fig. 5 compares the structure type of $ErPt_{3-x}Si_{1-y}$ ($x = 0.17$, $y = 0.16$; a_0, c_0) with the superstructure $Er_{36}Pt_{102-z}Si_{32}$ ($z = 2.61$, $= ErPt_{2.76}Si_{0.89}$; $a = a_0$, $c = 2c_0$; [5]), particularly for the "problematic area". Labeling of atoms in $Er_{36}Pt_{102-z}Si_{32-x}$ (Fig. 5b) adheres to Ref. [5]. Although the overall architecture of the two structure types is similar, the superstructure shows atom/vacancy ordering i.e. sites Pt8a and Pt9 (as labeled in Fig. 5a for the subcell) are unoccupied in the superstructure. All crystals studied in the present investigation do not show superstructure formation. The reason for the polymorphic transformation in the Er-containing compound is still an open scientific task as we

Table 3
Selected interatomic distances in the $TbPt_{3-x}Si_{1-y}$ compound ($|\Delta| < 0.004$ nm, cell parameters from XPD were used).

Tb1a-		Tb3-		Pt4-		Pt9-		Si1a-	
2 Pt7	0.286	4Pt4	0.294	2Si1a	0.240	1Pt10c	0.225	1Pt3	0.230
2 Si1a	0.288	8Pt1	0.295	2Pt1	0.284	2Si2	0.246	1Pt1	0.234
1Pt9	0.294			2Pt2	0.290	2Tb1b	0.252	2Pt4	0.240
2Pt3	0.295	Pt1-		1Tb3	0.294	1Pt8b	0.264	1Pt2	0.240
2Si3	0.309	1Si1a	0.234	2Pt1	0.300			2Tb1a	0.309
1Pt8b	0.309	2Pt4	0.284	1Tb2	0.305			2Tb2	0.317
1Pt4	0.316	2Tb3	0.295	1Tb1a	0.316	Pt10a-			
1Pt11	0.322	1Pt2	0.298	1Tb2	0.331	2Si2	0.257	Si1b-	
2Pt2	0.327	2Pt1	0.299			4Pt3	0.266	1Pt1	0.263
2Si2	0.338	2Pt4	0.301			1Pt8b	0.270	1Pt2	0.268
1Tb1b	0.364	2Tb2	0.313	Pt6-		2Pt6	0.298	2Pt4	0.271
				2Pt10c	0.271	2Tb2	0.306	2Tb2	0.299
Tb1b-		Pt2-		2Pt3	0.276	2Tb1b	0.312	2Tb1b	0.306
1Pt8b	0.266	1Si3	0.239	2Pt11	0.284				
2Pt7	0.266	1Si1a	0.240	2Pt2	0.291	Pt10b-		M5-	
2Pt3	0.287	2Pt4	0.290	4Tb2	0.307	2Si2	0.232	2Pt7	0.244
2Pt7	0.287	1Pt6	0.291			1Pt8b	0.235	2Pt8a	0.246
1Pt8a	0.290	2Pt11	0.292	Pt7-		4Pt3	0.268	2Pt3	0.255
1Pt10b	0.293	1Pt1	0.298	1Si3	0.237	2Tb1b	0.293	2Pt10b	0.259
2Si2	0.302	2Tb2	0.299	1M5	0.244	2Si2	0.295	4Tb1b	0.325
2Si1b	0.306	2Tb1a	0.327	2Tb1b	0.266	2Tb2	0.331		
2Si3	0.323			2Pt8a	0.282				
1Tb1b	0.350					Pt10c-		Si2-	
				Pt8a-		4Pt3	0.270	1Pt10b	0.232
Tb2-		Pt3-		2M5	0.246	2Pt6	0.271	2Pt7	0.245
1Pt10c	0.281	1M5	0.255	4Pt7	0.282	2Tb2	0.282	1Pt8a	0.255
2Pt3	0.298	2Pt10a	0.266	2M5	0.286	2Si2	0.287	2Pt3	0.261
2Pt2	0.299	1Pt6	0.276	2Tb1b	0.290	2Tb1b	0.337		
2Si1b	0.299	2Tb1b	0.287	1Pt10b	0.293				
1Pt4	0.305	2Tb2	0.298			Pt11-		Si3-	
2Pt6	0.307			1Pt8b-		2Si3	0.242	2Pt7	0.237
1Pt11	0.307			1Pt10b	0.235	2Pt6	0.284	2Pt2	0.239
2Pt1	0.313			2Si2	0.257	4Pt2	0.292	2Pt11	0.242
1Pt4	0.331			2Tb1b	0.266	2Tb2	0.307	4Tb1a	0.309
1Tb1a	0.384			4Pt7	0.291	2Tb1a	0.3226		

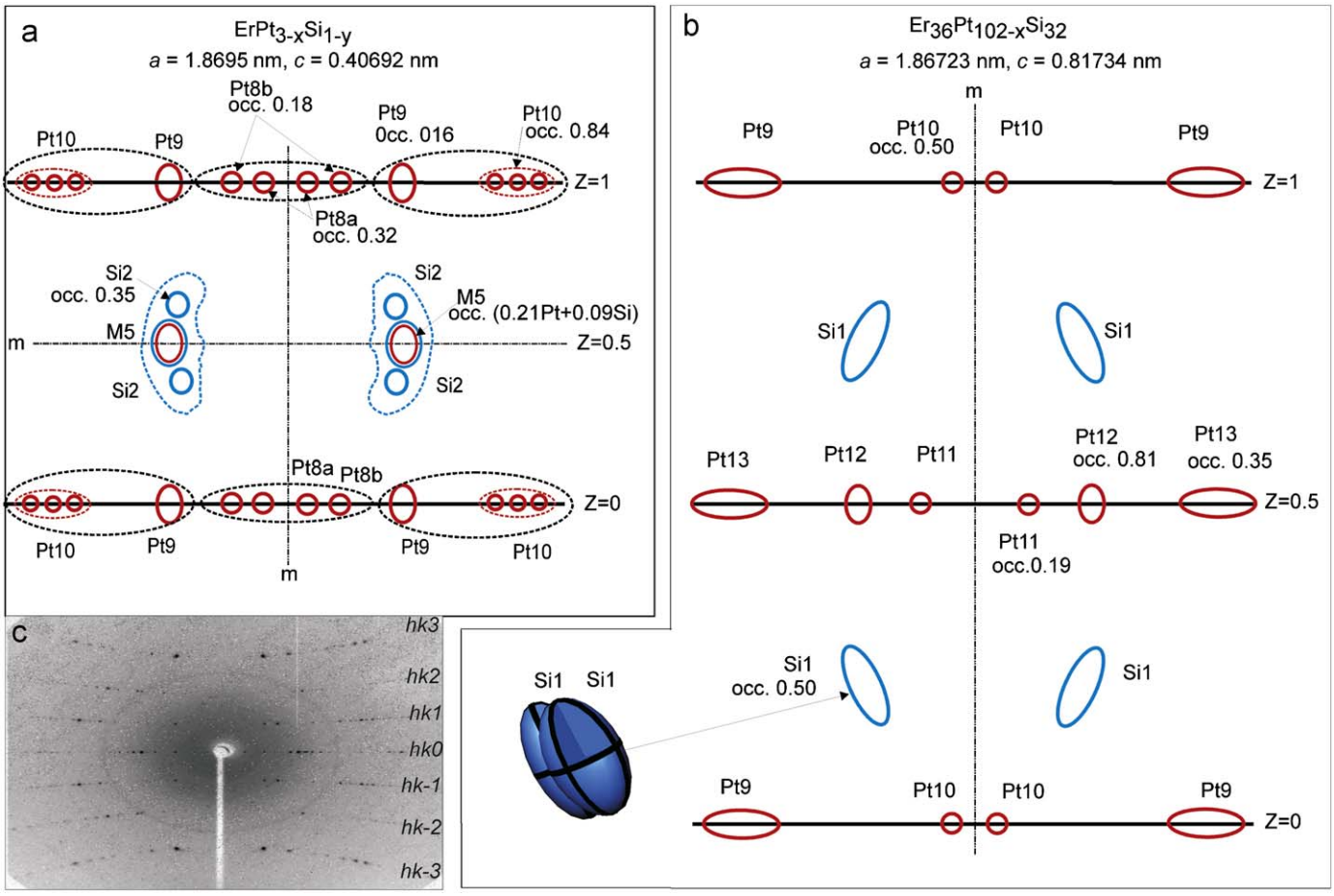

Fig. 5. Relations between (a) $ErPt_{3-x}Si_{1-y}$ (this work), (b) superstructure $Er_{36}Pt_{102-x}Si_{32}$ [5], and (c) presents the rotation photograph for $ErPt_{3-x}Si_{1-y}$ (rotation axis [001], note the absence of $c = 2c_0$ superstructure reflections). Groups of atoms corresponding to one "physical atom" are encircled by a dashed line. Labels for atoms in $Er_{36}Pt_{102-x}Si_{32}$ refer to Ref. [5]. For details see text.

have not yet studied a possible formation of superstructures in $RPt_{3-x}Si_{1-y}$ as a function of temperature, pressure, and/or stoichiometry. Only crystals of $DyPt_{3-x}Si_{1-y}$ from alloys annealed at 600 or 900 °C gave practically identical results.

4. Conclusion

All members of the series for $RPt_{3-x}Si_{1-y}$, R = Y, Tb, Dy, Ho, Er, Tm, Yb, adopt crystal structures of the same type (space group $P4/mbm$). The crystal structure of $RPt_{3-x}Si_{1-y}$ ($x \approx 0.17$–0.22, $y \approx 0.11$–0.16) is a packing of distorted $CePt_3B$-type building blocks, some of which exhibit a high degree of atom disorder at a slightly smaller amount of silicon and platinum than $CePt_3Si$. The present work suggests $Er_{36}Pt_{102-x}Si_{32}$ ($x = 2.61$, space group $P4_2/mnm$, $Z = 1$, $a = 1.86723$, $c = 0.81734$ nm), previously published with twice the c-parameter [5], to be a polymorphic modification of $ErPt_{3-x}Si_{1-y}$.

Acknowledgments

This research was supported by the Austrian National Science Foundation FWF project P18054-Phy. The authors are grateful to the Russian Foundation of Basic Research for support of the projects nos. 08–03–01072 and 06–03–90579 BNTS and to the bilateral WTZ Austria–Russia, project 17/2006.

Appendix A. Supplementary material

Supplementary data associated with this article can be found in the online version at doi:10.1016/j.jssc.2009.05.005.

References

[1] E. Bauer, G. Hilscher, H. Michor, C. Paul, E.W. Scheidt, A.V. Gribanov, Y.D. Seropegin, H. Noël, M. Sigrist, P. Rogl, Phys. Rev. Lett. 92 (2004) 027003/1–027003/4.
[2] M. Yogi, K. Kitaoka, S. Hashimoto, T. Yasuda, R. Settai, T.D. Matsuda, Y. Haga, Y. Onuki, P. Rogl, E. Bauer, Phys. Rev. Lett. 93 (2004) 027003/1–027003/4.
[3] S.S. Saxena, P. Mounthoux, Nature 427 (2004) 799.
[4] E. Bauer, R. Lackner, G. Hilscher, H. Michor, M. Sieberer, A. Eichler, A. Gribanov, Y. Seropegin, P. Rogl, J. Phys. Condens. Matter 17 (2005) 1877–1888.
[5] A.I. Tursina, A.V. Gribanov, H. Noél, P. Rogl, Y.D. Seropegin, Acta Crystallogr. Sect. E Struct. Rep. Online 60 (2) (2004) i8–i9.
[6] A.I. Tursina, A.V. Gribanov, H. Noél, P. Rogl, Y.D. Seropegin, J. Alloys Compd. 395 (2005) 93–97.
[7] E. Bauer, R. Lackner, G. Hilscher, H. Michor, E.-W. Scheidt, W. Scherer, P. Rogl, A. Gribanov, A. Tursina, Y. Seropegin, G. Giester, Phys. Rev. B Condens. Matter Mater. Phys. 73 (10) (2006) 104405.
[8] O.L. Borisenko, O.I. Bodak, Y.D. Seropegin, V.N. Nikiforov, M.V. Kovachikova, Y.V. Kochetkov, Izvestia Akad. Nauk SSSR Metally 2 (1995) 167–172 (in Russian).
[9] A. Gribanov, A. Grytsiv, E. Royanian, P. Rogl, E. Bauer, G. Giester, Y. Seropegin, J. Solid State Chem. 181 (11) (2008) 2964–2975.
[10] Nonius Kappa CCD Program Package COLLECT, DENZO, SCALEPACK, SORTAV. Delft, The Netherlands, Nonius, 1998.
[11] G.M. Sheldrick, Acta. Crystallogr. A64 (2008) 112–122.
[12] T. Roisnel, J. Rodriguez-Carvajal, Materials science forum, in: Proceedings of the European Powder Diffraction Conference (EPDIC7), 2000, pp. 118–123.